

Detection of somatic quantitative genetic alterations by multiplex polymerase chain reaction for the prediction of outcome in diffuse large B-cell lymphomas

Fabrice Jardin,^{1,2} Philippe Ruminy,¹ Jean-Pierre Kerckaert,³ Françoise Parmentier,¹ Jean-Michel Picquenot,¹ Sabine Quief,³ Céline Villenet,³ Gérard Buchonnet,¹ Mario Tosi,⁴ Thierry Frebourg,⁴ Christian Bastard,¹ and Hervé Tilly^{1,2}

¹INSERM U618, European Institute of Peptide Research (IFR23), Rouen; ²Centre Henri Becquerel, Department of Hematology, Rouen; ³INSERM U837, Université de Lille 2, IFR 114 and from the Institut de Recherches sur le Cancer, Lille; ⁴INSERM U614, Institut Hospitalo-Universitaire de Recherche, Rouen, France

Acknowledgments: the authors thank Gregory Raux, Vincianne Rainville, Claude Lamarche, and Marie Cornic for their technical support.

Funding: this work was supported by grants from the Comité de L'Eure de la Ligue contre le Cancer and from Le canceropole Nord-Ouest.

Manuscript received September 17, 2007. Revised version arrived on October 29, 2007. Manuscript accepted November 22, 2007.

Correspondence: Fabrice Jardin, Department of Hematology, Centre Henri Becquerel, 76000 Rouen, France. E-mail: fabrice.jardin@rouen.fnclcc.fr

The online version of this article contains a supplemental appendix.

ABSTRACT

Background

Genomic gains and losses play a crucial role in the development of diffuse large B-cell lymphomas. High resolution array comparative genomic hybridization provides a comprehensive view of these genomic imbalances but is not routinely applicable. We developed a polymerase chain reaction assay to provide information regarding gains or losses of relevant genes and prognosis in diffuse large B-cell lymphomas.

Design and Methods

Two polymerase chain reaction assays (multiplex polymerase chain reaction of short fluorescent fragments, QMPSF) were designed to detect gains or losses of *c-REL*, *BCL6*, *SIM1*, *PTPRK*, *MYC*, *CDKN2A*, *MDM2*, *CDKN1B*, *TP53* and *BCL2*. Array comparative genomic hybridization was simultaneously performed to evaluate the sensitivity and predictive value of the QMPSF assay. The biological and clinical relevance of this assay were assessed.

Results

The predictive value of the QMPSF assay for detecting abnormal DNA copy numbers ranged between 88-97%, giving an overall concordance rate of 92% with comparative genomic hybridization results. In 77 cases of diffuse large B-cell lymphomas, gains of *MYC*, *CDKN1B*, *c-REL* and *BCL2* were detected in 12%, 40%, 27% and 29%, respectively. *TP53* and *CDKN2A* deletions were observed in 22% and 36% respectively. *BCL2* and *CDKN2A* allelic status correlated with protein expression. *TP53* mutations were associated with allelic deletions in 45% of cases. The prognostic value of a single QMPSF assay including *TP53*, *MYC*, *CDKN2A*, *SIM1* and *CDKN1B* was predictive of the outcome independently of the germinal center B-cell like/non-germinal center B-cell like subtype or the International Prognostic Index.

Conclusions

QMPSF is a reliable and flexible method for detecting somatic quantitative genetic alterations in diffuse large B-cell lymphomas and could be integrated in future prognostic predictive models.

Key words: deletions, gains, diffuse large B-cell lymphoma, prognosis.

Citation: Jardin F, Ruminy P, Kerckaert J-P, Parmentier F, Picquenot J-M, Quief S, Villenet C, Buchonnet G, Tosi M, Frebourg T, Bastard C, and Tilly H. Detection of somatic quantitative genetic alterations by multiplex polymerase chain reaction for the prediction of outcome in diffuse large B-cell lymphomas. Haematologica 2008;93(4):543-550. doi: 10.3324/haematol.12251

©2008 Ferrata Storti Foundation. This is an open-access paper.

Introduction

Diffuse large B-cell lymphomas (DLBCL) account for approximately one third of all non-Hodgkin's lymphomas in Western countries.¹ These neoplasms have a common aggressive clinical behavior but display great heterogeneity. The underlying molecular basis of this heterogeneity was partially elucidated by gene expression profiling studies that identified three major subgroups of DLBCL, termed germinal center B-cell-like DLBCL (GCB-DLBCL), activated B-cell-like DLBCL (ABC-DLBCL) and primary mediastinal DLBCL.^{2,3} Malignant lymphomas, and especially DLBCL, are genetically characterized by recurring translocations, such as t(3;14)(q27;q32), t(8;14)(q24;q32), or t(14;18)(q32;q21), deregulating the *BCL6*, *MYC* and *BCL2* genes respectively as a result of their juxtaposition to immunoglobulin genes.⁴ Transgenic mouse models with deregulated expression of *BCL6* or *MYC* develop tumors displaying features of DLBCL or human Burkitt's lymphoma respectively.^{5,6} However, aberrant expression of *BCL2* is not sufficient in mice for full lymphoma transformation and t(14;18) or t(3;14) are observed in non-tumoral B cells, indicating that accumulation of other genetic alterations is required for the malignant transformation.^{7,8} Array-based comparative genomic hybridization (array CGH) has the potential to detect these additional aberrations that play an important role in the development and progression of lymphomas. Using this approach, it was shown that recurrent genomic imbalances are related to the cell of origin or correlated with the prognosis.⁹⁻¹² However, an array-CGH approach is not routinely applicable. By contrast, quantitative multiplex polymerase chain reaction of short fluorescent fragments (QMPSF) is an inexpensive and sensitive method for the detection of genomic deletions or duplications based on the simultaneous amplification of short genomic fragments using dye-labeled primers under quantitative conditions.¹³⁻¹⁵ Using this approach, we determined gain/loss frequencies of several targeted genes and built a biological score able to predict the outcome of DLBCL independently of the International Prognostic Index.

Design and Methods

Patients

Seventy-seven patients diagnosed with a DLBCL (76 nodal cases and one extra-nodal case) followed in our institution were selected. This study was approved by the ethics committee of our institution. The inclusion criteria were the availability of appropriate paraffin embedded-tissues, available tumor DNA at the time of diagnosis from fresh or frozen tissues and complete clinical data. The median age of the patients was 58 years

(range, 17 to 87 years). The distribution according to International Prognostic Index scores was as follows: scores 0-1=27 (36%); 2-3 = 30 (40%); 4-5 = 18 (24%). All patients received an anthracycline-containing combination of chemotherapy, including CHOP (40%) or intensified CHOP (39%) regimens. Eight patients received rituximab combined with chemotherapy as first line treatment and 13 received intensified chemotherapy with autologous stem cell transplantation in first response.

Array CGH

The CGH analysis was performed using a high resolution 60-mer oligonucleotide-based microarray that contains ~43,000 probes, with an average spatial resolution of 35 kB (Human genome CGH array 44B, Agilent Technologies, CA, USA). High molecular weight DNA was prepared using the standard method. Restriction was performed as recommended by the manufacturer of the arrays. Tumor DNA was labeled with cyanine-5 (Cy5) and reference DNA (pooled normal DNA, Promega, Madison, WI, USA) was labeled with cyanine-3 (Cy3). To increase the probability of detecting relevant genomic gains or losses involving candidate genes related to the outcome of DLBCL, CGH was performed in 17/77 cases selected on the basis of their particularly unfavorable outcome. The analyses of microarray images were performed with the Agilent CGH analytics 3.4.27 software. Classification as gain or loss was based on identification as such by the CGH plotter and visual inspection of the log₂ ratios. Signal log₂ ratios greater than 0.25 or less than -0.25 were considered to indicate gains and losses, respectively.

QMPSF assay

QMPSF is a sensitive method for detecting genomic deletions or duplications based on the simultaneous amplification of short genomic fragments using dye-labeled primers under quantitative conditions (patent FR 020924).^{13,14,16} Polymerase chain reaction (PCR) products were analyzed on a sequencing platform used in the fragment analysis mode in which both peaks heights and areas are proportional to the quantity of template present for each target sequence. We designed two distinct QMPSF assays which contain the following target genes: Assay 1 - *MYC* (8q24), *TP53* (17p13), *CDKN2A* (9p21), *SIM1* (6q16) and *CDKN1B* (12p13.1); Assay 2 - *c-REL* (2p13), *BCL6* (3q27), *PTPRK* (6q22), *BCL2* (18q21) and *MDM2* (12q15). The *CECR1* gene, located at 22q11 was chosen as a reference gene, considering the fact that it appears uncommonly affected by aneuploidy or focal gains or losses in our own cytogenetic database and in published DLBCL series.^{12,17,18} Primer pairs were designed for each of these 11 genes to generate PCR fragments ranging from 150 to 250 base pairs and chosen in a way that they do not encompass polymorphisms (*Online Supplemental Table S1*). PCR were run from 100 ng of genomic DNA in a final volume of 25 μ L with 0.16

mmol/L of each deoxynucleoside triphosphate, 1.5 mmol/L MgCl₂, 1 unit of thermoprime Plus DNA polymerase (AB gene, Epson, United Kingdom), 5% DMSO and 0.5 to 1.6 µmol/L of each primer, one primer of each pair carrying a 6-FAM label. After initial denaturation for 3 min at 94°C, 20 cycles were performed consisting of denaturation, 94°C for 15 sec, annealing 90°C for 15 sec (ramping 3°C/sec) and extension 70°C, 15 sec (ramping 3°C/sec, followed by a final extension step for 5 min at 70°C). Two control DNA were used (commercial DNA, Roche and a DNA extracted from a reactive lymph node) to calculate the mean normal/tumoral peak height ratio. Using this approach, we demonstrated that *TP53* and *MDM2* somatic defects could be reliably detected when the proportion of tumoral cells was as low as 20%.¹⁵ In addition, polymorphic gene copy number changes were excluded in some cases using matched non-tumoral DNA as control.

QMPSF validation

Considering array-CGH as the reference method, QMPSF and array CGH were both performed in 17 cases. A correlation between CGH log₂ and QMPSF ratio was established and allowed the sensitivity, specificity, positive and negative predictive values of the QMPSF assay to be determined. To determine the reliable QMPSF ratio for detecting gene gains or losses, the equation of the regression curve obtained was used to deduce the QMPSF ratio cut-offs corresponding to a CGH log₂ ratio of -0.25 (loss) and +0.25 (gain).

TP53 mutational status

To investigate the frequency of *TP53* mutations, the highly conserved exons 5 to 8 (central core domain) were screened for the mutation, as described elsewhere.¹⁹

Immunohistochemistry

Immunohistochemical studies were performed on formalin-fixed, paraffin-embedded tissue sections of lymph node (n = 76) or spleen tissue (n = 1) using antibodies directed against BCL2, p53 (Dako), BCL6, p27 (Novacastra), p16 (Biocare Medical), and c-REL (Calbiochem). Cases were classed as expressing BCL2 and c-REL if the protein was detected in > 50% tumor cells, and p27 and p16 positive if the protein was detected in > 10% tumor cells. GCB and non-GCB phenotypes were defined using the decision tree established by Hans with the same cut-offs.²⁰

Statistic analysis

The linear relationship between QMPSF ratio and CGH fluorescence ratio was established using Pearson's coefficient (R). Overall survival was measured from the time of diagnosis to the date of death or last follow-up alive. Progression-free survival was calculated from the initiation of the treatment to the date

of relapse, progression or death from any cause. Progression-free survival and overall survival rates were estimated by the Kaplan-Meier method and statistical differences were assessed by the log-rank test. A Fisher's exact test was used to evaluate the unequal distribution of the different genetic abnormalities and the GCB/ non-GCB phenotype and to correlate protein expression and allelic status. A multivariate analysis using a Cox model was conducted to assess the independent prognostic influence of the International Prognostic Index and QMPSF score. Analyses were performed using StatView® and SEM software.²¹

Results

Array CGH

Chromosomal alterations were observed in all cases. The most frequent imbalances were loss of 7q31.33 (60%), loss of 9p21 (60%), loss of 14q23.1 (60%), loss of 14q23.1 (60%), loss of 13q33.3 (50%) loss of 6q14-q22 (50%), loss of 5q12.3 (40%), loss of 17p13.2 (25%), loss of 2q24 (35%), gains of 18q21.2 (60%) and 18q22.3 (30%), gain of 1q21-23 (50%), gain of 19q13.33-q13.41 (40%), gain of chromosome 12 (40%), gain of 2p14-p16 (25%), gain of 6p (25%), and gain of 8q24.12-q24.21 (20%) (*Online Supplemental Figure S1*).

QMPSF assays

QMPSF and CGH experiments were both performed in 17 cases (Figure 1). The linear correlation between CGH log₂ ratio and QMPSF ratio is illustrated in Figure 2A. The R² coefficient was 0.70, indicating a good concordance between the results of the two experiments. From the curve equation, a gene loss, defined by a mean CGH log₂ ratio < -0.25, corresponds to a QMPSF ratio below 0.83. A gain detected by a mean CGH log₂ ratio > +0.25 corresponds to a QMPSF ratio above 1.13. To maximize detection of true losses and gains, the ratio values finally used were 0.7 and 1.2, respectively. With these cut-offs, DNA copy number changes were confirmed in 156/170 amplicons, giving an overall concordance rate of 92%. The positive and negative predictive values of QMPSF for detecting gains were 88% and 97%, respectively. Similarly, the positive and negative predictive values of QMPSF for detecting gene losses were 90% and 97%, respectively.

Allelic deletion of *CDKN2A* was detected in 9/17 cases using both methods, giving a concordance rate of 100%. Array CGH analysis indicated that loss of *CDKN2A* gene copy number could result from either a large deletion encompassing the telomeric part of the short arm of chromosome 9 or could be the consequence of a narrow deletion. In 6/9 cases, a CGH log₂ ratio < -1.0 indicated a homozygous deletion of *CDKN2A*, corresponding to a QMPSF ratio lower than 0.45 in all cases (Figure 2).

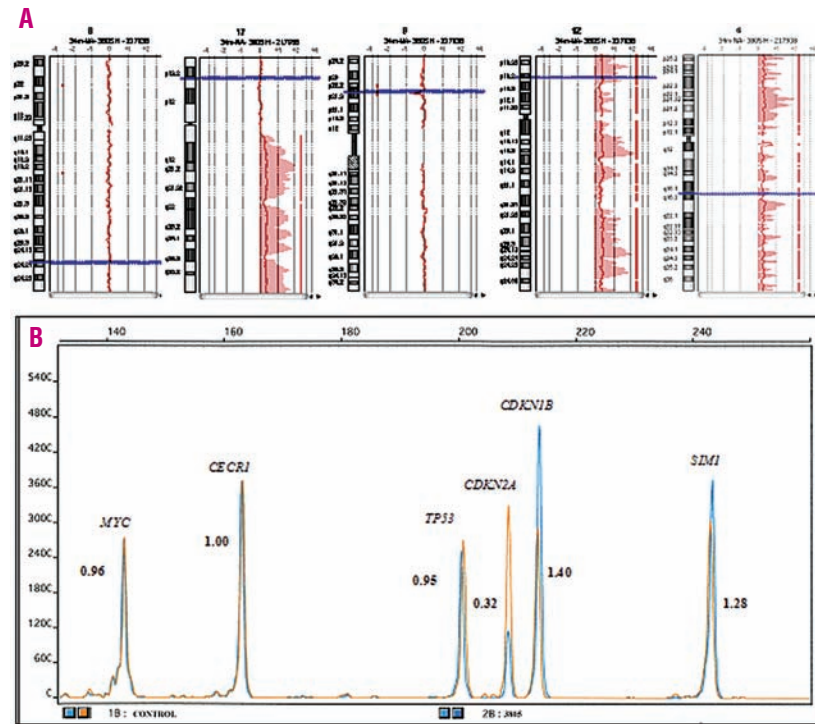


Figure 1. Results of QMPSF and CGH experiments in a single DLBCL case (A) Array CGH shows (from the left to the right) a chromosome 8 in germline configuration, a gain of the long arm of chromosome 17, a short deletion of the 9p21 band, trisomy 12 and trisomy 6. Horizontal blue lines on the chromosome pictogram indicate the location of the five genes included in the QMPSF assay. (B) The corresponding QMPSF assay enables, in a single PCR assay, the detection of gains or losses of gene copy numbers of *MYC* (8q24), *TP53* (17p13), *CDKN2A* (9p21), *CDKN1B* (12p13), and *SIM1* (6q16). Tumor and normal DNA electropherograms are indicated in blue and orange, respectively. Amplicons are separated and identified by their respective expected sizes (indicated on the upper abscissa). Peak height ratios between tumor and normal DNA are indicated for each gene. *CERC1*, located on chromosome 22 is used as the reference gene to normalize peak ratios (1.00). *MYC* and *TP53* QMPSF ratios indicated no gene copy number abnormality. A decrease of the QMPSF *CDKN2A* ratio below a cut-off of 0.7 (0.32) corresponds to the 9p21 loss detected by CGH. In contrast, trisomy 12 and 6 are detected by an increase of the QMPSF ratios (>1.2) of *CDKN1B* and *SIM1*, respectively.

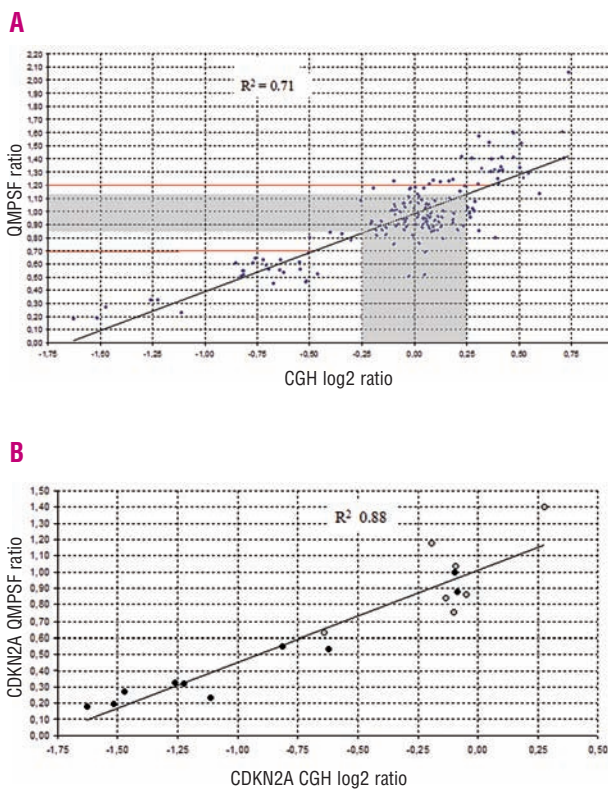


Figure 2. Correlation between the QMPSF assay and CGH experiments in *de novo* DLBCL (A) The correlation curve obtained was used to deduce the most reliable minimal QMPSF ratio cut-offs corresponding to a CGH log₂ ratio of -0.25 and +0.25 (gray areas) to detect gene losses and gains, respectively. To maximize detection of true gene copy number changes, QMPSF ratio cut-offs of 0.7 and 1.2 were finally used (horizontal red lines). (B) Correlation between the QMPSF assay and CGH experiments for the *CDKN2A* gene. Coding *CDKN2A* gene protein (p16ink4a) detected by immunohistochemistry is indicated for each individual cases (positive cases, gray dots; negative cases, black dots).

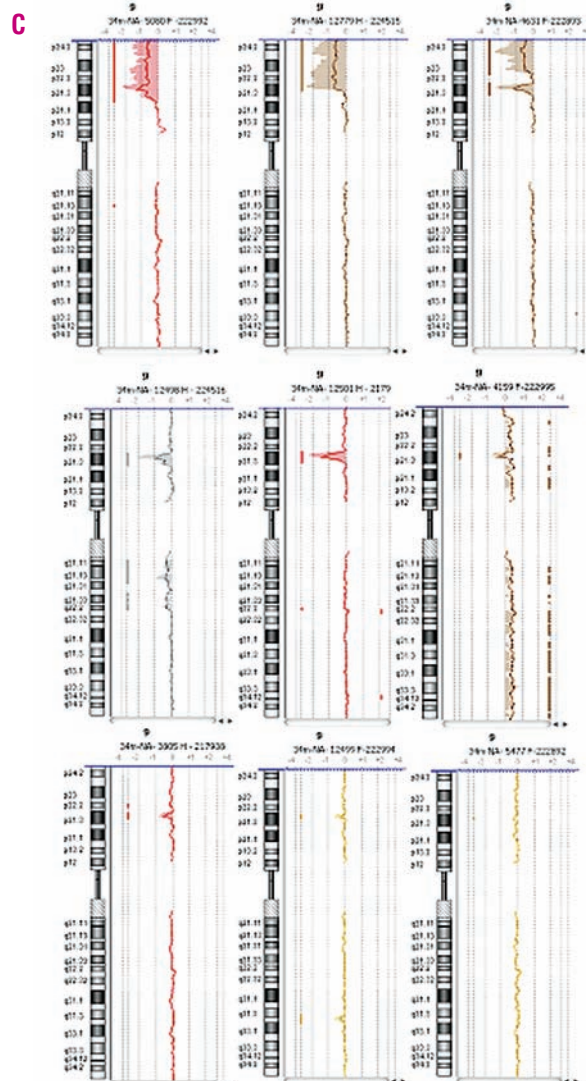


Table 1. Allelic status assessed by QMPFSF in DLBCL and correlation with protein expression assessed by immunohistochemistry and GCB / non GCB subtypes.

| Gene | Protein | Allelic status (%) | Positive protein expression (%) | GCB subtype (%)/non-GCB subtype (%) | protein expression ^a | Fisher's p GCB vs non-GCB ^b | |
|--------|---------|--------------------|---------------------------------|-------------------------------------|---------------------------------|--|--------|
| TP53 | p53 | germline | 58 (75.3) | 11 (19) | 24 (41.4) / 34 (58.6) | 0.74 | 0.78 |
| | | gain | 1 (1.3) | 0 | 0 (0) / 1 (100) | | |
| | | loss | 18 (23.4) | 5 (27.8) | 7 (38.9) / 11 (61.1) | | |
| CDKN2A | p16 | germline | 49 (63.6) | 18 (36.7) | 23 (46.9) / 26 (53.1) | 0.0031 | 0.15 |
| | | gain | 1 (1.3) | 1 (100) | 0 (0) / 1 (100) | | |
| | | loss | 27 (35.1) | 3 (11.1) | 8 (29.6) / 19 (70.4) | | |
| CDKN1B | p27 | germline | 46 (58.4) | 13 (28.2) | 20 (43.5) / 26 (56.5) | 0.45 | 0.81 |
| | | gain | 30 (40.2) | 11 (36.7) | 11 (36.7) / 19 (63.3) | | |
| | | loss | 1 (1.3) | 1 (100) | 0 (0) / 1 (100) | | |
| MYC | MYC | germline | 65 (84.4) | 30 (46.9) | 24 (36.9) / 41 (63.1) | 0.19 | 0.0816 |
| | | gain | 10 (12) | 7 (70) | 7 (70) / 3 (30) | | |
| | | loss | 2 (2.6) | 0 | 0 / 2 (100) | | |
| SIM1 | SIM1 | germline | 48 (63.6) | ND | 24 (50) / 24 (50) | - | 0.05 |
| | | gain | 1 (1.3) | ND | 0 (0) / 1 (100) | | |
| | | loss | 28 (36.4) | ND | 7(25) / 21 (75) | | |
| c-REL | REL | germline | 56 (72.7) | 13 (27) | 18 (32.1) / 38 (67.9) | 0.55 | 0.02 |
| | | gain | 21 (27.3) | 7 (36.8) | 13 (61.9) / 8 (38.1) | | |
| | | loss | 0 | - | - | | |
| BCL2 | BCL2 | germline | 54 (70.1) | 15 (27.8) | 26 (48.2) / 28 (51.8) | 0.0003 | 0.042 |
| | | gain | 23 (29.9) | 17 (73.9) | 5 (21.7) / 18 (78.3) | | |
| | | loss | 0 | - | - | | |
| BCL6 | BCL6 | germline | 57 (74) | 37 (64.9) | 27 (47.4) / 30 (52.6) | 0.39 | 0.047 |
| | | gain | 16 (20.8) | 8 (50) | 3 (18.8) / 13 (81.3) | | |
| | | loss | 4 (5.2) | 2 (50) | 1 (25) / 3 (75) | | |
| MDM2 | MDM2 | germline | 49 (63.6) | ND | 19 (38.8) / 30 (61.2) | - | 0.47 |
| | | gain | 26 (33.8) | ND | 12 (46.2) / 14 (53.8) | | |
| | | loss | 2 (2.6) | ND | 0 (0) / 2 (100) | | |
| PTPRK | PTPRK | germline | 57 (74) | ND | 29 (50.9) / 28 (49.1) | - | 0.0047 |
| | | gain | 3 (3.9) | ND | 0 (0) / 3 (100) | | |
| | | loss | 17 (22.1) | ND | 2 (11.8) / 15 (88.2) | | |

^aCorrelation between allelic status and protein expression; ^bcomparison frequencies of gains or losses according to GCB/non-GCB subgroups.

Frequencies of gain and loss in the overall DLBCL population

Gain and loss frequencies of the ten genes analyzed by the two QMPFSF assays are indicated in Table 1. Some target genes were mainly gained such as *MYC*, *CDKN1B*, *MDM2*, *c-REL*, or *BCL2*. By contrast, *CDKN2A*, *TP53*, *SIM1* and *PTPRK* were almost exclusively deleted. *CDKN2A* loss was observed in 36% of DLBCL. In 13 cases, the QMPFSF ratio was below 0.45, corresponding to a CGH log₂ ratio < -0.5, indicating a homozygous deletion. *SIM1* (6q16) and *PTPRK* (6q22) deletions were more frequently observed in MUM1-positive DLBCL ($p=0.004$ and 0.008 , respectively) and in the non-GCB DLBCL subgroup. *c-REL* gains were observed in 13/31 (42%) GCB-DLBCL and in 8/46 (17%) non-GCB DLBCL ($p=0.02$). Gain of *BCL2* copy was more frequently observed in the non-GCB subtype. Among the 13 cases with homozygous *CDKN2A* deletion, 11 belonged to the non-GCB subtype, and two to the GCB subtype ($p=0.06$). However, some simultaneous gene copy number abnormalities also occurred frequently in the same tumors, even if these gene are not located on the same chromosome. For instance, 11/16 cases (68%) with *BCL6* (3q27) gains also had *BCL2*

(18q21) gains ($p=0.0003$). Multiple losses of tumor suppressor genes can be observed. For instance, in five cases (6%), concomitant loss of *TP53* and *CKND2A* was observed. Furthermore, *CDKN2A* allelic loss was associated with *SIM1* and *PTPRK* deletions ($p=0.003$). The details of allelic status of each gene are indicated in the supplemental data (*Online Supplemental Table S2*). Furthermore, using matched non-tumoral DNA as a control, we confirmed that gene copy number changes were not inherited polymorphisms (*data not shown*).

Protein expression, TP53 mutation and allelic status

The lack of p16 protein expression was mainly observed in cases characterized by a *CDKN2A* QMPFSF ratio <0.7 (Figure 2B and Table 1). Conversely, gain of *BCL2*-gene copy number correlated positively with a higher proportion of BCL2-positive cases. A trend for higher MYC protein expression was observed in cases of gain of *MYC* copies. *c-REL* expression was detected by immunohistochemistry in seven of the 21 cases (33%) that displayed *c-REL* gains. Most of the cases (6/7) with both *c-REL* gain and *c-REL* protein expression were classified in the GCB subtype, as compared to only one case classified in the non-GCB subtype

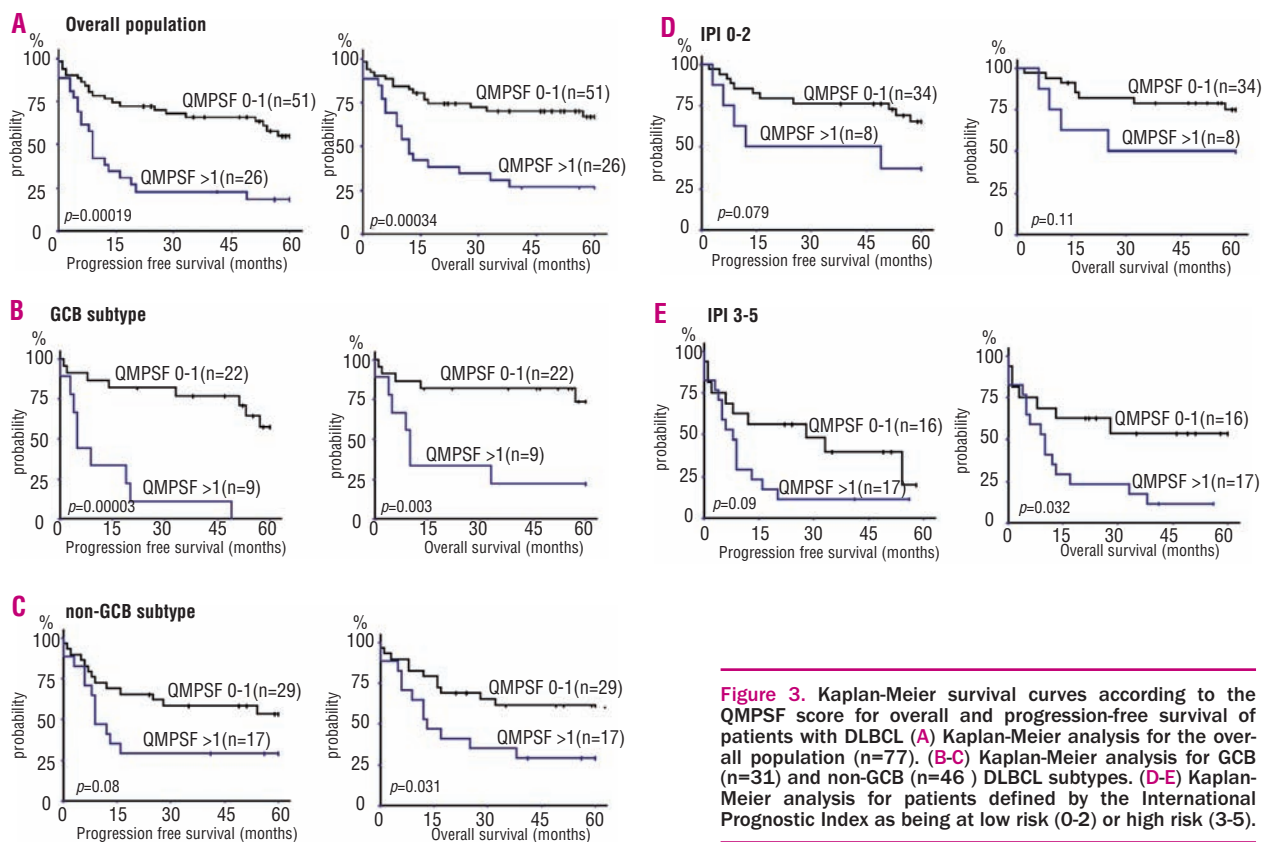


Figure 3. Kaplan-Meier survival curves according to the QMPSF score for overall and progression-free survival of patients with DLBCL (A) Kaplan-Meier analysis for the overall population (n=77). (B-C) Kaplan-Meier analysis for GCB (n=31) and non-GCB (n=46) DLBCL subtypes. (D-E) Kaplan-Meier analysis for patients defined by the International Prognostic Index as being at low risk (0-2) or high risk (3-5).

(Table 1). *TP53* sequence analysis revealed 11 missense single-base substitutions and one nonsense mutation, distributed in 77 patients. In 5/11 cases, *TP53* missense mutations were associated with allelic loss. Overall, cases with allelic loss tended to be more frequently mutated (5/18), as compared to tumors with no *TP53* deletion (6/59) ($p=0.11$). p53 protein accumulation was detected by immunohistochemistry in 7/11 mutated cases and in the 4/5 cases with both *TP53* mutations and deletions (Online Supplemental Table S3). By contrast, only 9/57 unmutated cases (15%) expressed p53, indicating a strong correlation between *TP53* mutations and p53 expression ($p=0.001$).

Prognostic significance of QMPSF assays

The prognostic value of the QMPSF assays was analyzed for each individual gene or using a scoring system established as the amount of gene number abnormalities detected by a single QMPSF assay. Only gain of *CDKN1B* (12p13.1) was related to significantly shorter progression-free and overall survival. The 3-year progression-free survival rate was 34% for patients with gain of *CDKN1B*, (16-46% CI-95%), and 67% (52-79%, CI-95%) for patients with a germline configuration ($p=0.001$). Given the fact that tumor behavior is considered to be the result of multiple gene alterations, we assessed the additive or synergic effect of each gene gain or loss determined by a single QMPSF assay. Each abnormality was scored as +1 and was included in a scoring system. The addition of four abnormalities,

MYC and *CDKN1B* gains, *TP53* and *CDKN2A* losses, was the most powerful scoring system to predict the outcome. The progression-free and overall survival were significantly shorter for patients with a QMPSF score >1 than for patients whose tumors were scored 0-1. This prognostic value held true for the GCB and the non-GCB subtypes. The score remained significantly predictive of a shorter overall survival in the high risk group and tended to be predictive in the low risk group (Figure 3). The prognostic value of the score also held true when only patients treated with CHOP/CHOP-like regimens (excluding patients treated with autologous stem cell transplantation or rituximab as frontline therapy) were considered. In this subgroup (n=58), the 3-year progression-free survival rate was 64% (48-77%, CI-95%) for patients with a score of 0-1 and 16% (5-38%, CI-95%) for patients with a high QMPSF score ($p<0.001$). Similarly, the 3-year overall survival rate was 67% (51-79%, CI-95%) for the low score QMPSF group and 26% (12-49%, CI-95%) for patients with a score >1 ($p=0.001$).

A multivariate analysis was performed including International Prognostic Index, QMPSF score and the GCB/non-GCB status. In this model, with variables available for 75 patients, QMPSF was a strong predictor of both progression-free and overall survival ($p=0.0084$) along with the International Prognostic Index ($p=0.0059$). Finally, International Prognostic Index and QMPSF were integrated to build a composite score and defined three distinct prognostic groups (Figure 4).

Discussion

With the aim of providing a more accessible approach than array CGH, we developed a QMPSF assay for DLBCL. This method has several advantages in comparison to conventional or array CGH. Firstly, the QMPSF assay is a simple, routinely applicable and inexpensive method which requires only a minimal amount of tumor DNA for the simultaneous detection of genomic deletions or gains. Standardization of this method for a wide range of applications in molecular diagnostic laboratories is now conceivable and it should be integrated with others prognostic biomarkers. In contrast to array CGH, this inexpensive method can be used to determine rapidly the frequency of gains or losses of targeted oncogenes or tumor suppressor genes in large cohorts of patients. Secondly, QMPSF is a very flexible method which can be easily upgraded by changing targeted genes or can be dedicated specifically to distinct subtypes of non-Hodgkin's lymphoma. Thirdly, conventional CGH and to a lesser extent array CGH give information regarding the whole genome but are still limited by their level of resolution, which corresponds to regions encompassing dozens to hundreds of genes. By contrast using a QMPSF assay, indications regarding gains or losses of a limited number of key genes are obtained at the gene resolution level. However, it should be noted that QMPSF and CGH methods are both dependent on the proportion of tumor cells and may, therefore, be inadequate for detecting somatic defects only present in minor subclones.

Previous studies have reported comparative genome analyses of DLBCL, showing relevant differences in the genomic imbalance patterns of the activated B-cell-like and GCB subgroups.^{10,18,22} In the present study, we confirmed most of the genomic imbalances previously reported. For instance, it was recently shown that 6q21-22 losses, and 3q27 or 18q21-22 gains were more frequently observed in the activated B-cell-like subtypes, corresponding to *PTPRK* loss, and *BCL6* or *BCL2* gains, respectively, detected by QMPSF.¹⁰ A gain of *c-REL* copy number was observed in 29% of cases, a rate similar to that detected by CGH or by Southern blot.²³⁻²⁵ This gain is predominantly but not exclusively observed in the GCB subtype.^{2,22} Interestingly, *c-REL* copy number gain tends to be more frequently associated with protein expression only in the GCB subtype, indicating that *c-REL* protein deregulation pathways may be distinct in the two DLBCL subtypes. This observation was recently suggested by the correlation between chromosomal copy number changes and mRNA levels, revealing that genomic copy number gains in 2p14-16, 12q12-15, 3q27-qter and 18q21-q22 lead to subtype-specific up-regulation of genes located in these regions.¹⁰

Deletions of the *CDKN2A* gene were detected in 36% of the DLBCL cases. Tagawa and co-workers reported a more frequent loss of 9p21 in the activated B-cell-like

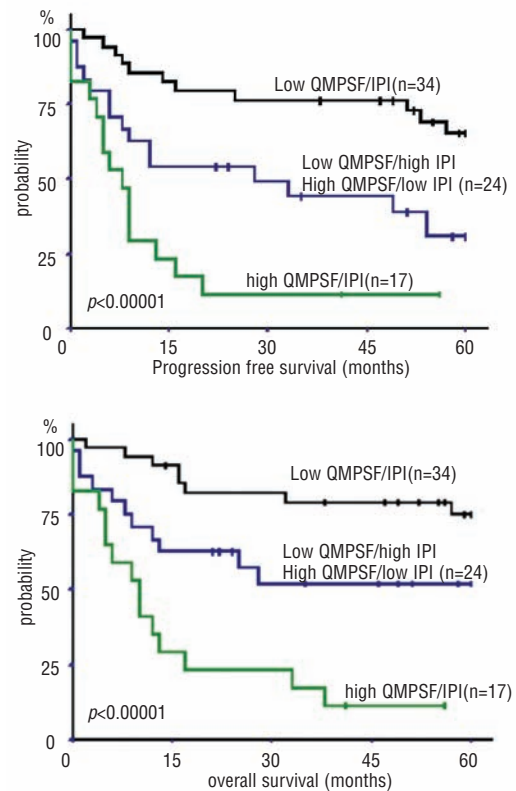


Figure 4. Impact of QMPSF/IPI combined score on survival of patients with DLBCL. International Prognostic Index (IPI) and QMPSF scores define three prognostic groups with different prognoses. The group with a favourable prognosis includes patients with both low QMPSF and IPI scores (n=34). The group with an unfavourable prognosis is defined by patients with both high QMPSF and IPI scores (n=17). The intermediate group comprises patients with low IPI/ high QMPSF scores or high IPI/QMPSF scores (n=24).

group.¹¹ Here we demonstrated at the gene resolution level that 9p21 loss detected by CGH involved the *CDKN2A* gene. The lack of p16^{ink4a} protein expression most frequently observed in cases of gene deletion indicated that this mechanism contributes, possibly in combination with methylation, to the down-regulation of this tumor suppressor gene.

To determine the biological relevance of *TP53* deletions detected by QMPSF, *TP53* mutation status of the central core binding domain was simultaneously assessed. Interestingly, as reported in a large series of NHL of various histology, we observed that *TP53* mutations were mainly present in tumors in which allelic loss had occurred.²⁶ This observation indicates that p53 mutations play both recessive and dominant roles in lymphoma.

We demonstrated that a single PCR assay, based on the gene copy numbers of *TP53*, *MYC*, *CDKN2A* and *CDKN1B*, had a prognostic value independent of the International Prognostic Index and added to its predictive power. A validation of our QMPSF score in an independent set of patients treated uniformly with regimens including rituximab is now necessary. It is likely that genes that are predictive in DLBCL mainly treated first

line without rituximab will have a different impact in patients treated with rituximab plus chemotherapy.^{27,28} Because our approach is very flexible, the QMPFSF assay can be easily upgraded and adapted to incorporate additional genes more predictive in this setting. For instance, it was shown that patients whose tumors have 3p11-12 gains have a worse prognosis and new potential tumor suppressor genes have been recently identified.^{10,29} These data should be integrated to establish a second generation QMPFSF assay to predict the outcome of lymphoma treated by immunochemotherapy.

References

1. Fisher SG, Fisher RI. The epidemiology of non-Hodgkin's lymphoma. *Oncogene* 2004;23:6524-34.
2. Rosenwald A, Wright G, Chan WC, Connors JM, Campo E, Fisher RI, et al. The use of molecular profiling to predict survival after chemotherapy for diffuse large-B-cell lymphoma. *N Engl J Med* 2002;346:1937-47.
3. Rosenwald A, Wright G, Leroy K, Yu X, Gaulard P, Gascoyne RD, et al. Molecular diagnosis of primary mediastinal B cell lymphoma identifies a clinically favorable subgroup of diffuse large B cell lymphoma related to Hodgkin lymphoma. *J Exp Med* 2003;198:851-62.
4. Willis TG, Dyer MJ. The role of immunoglobulin translocations in the pathogenesis of B-cell malignancies. *Blood* 2000;96:808-22.
5. Cattoretti G, Pasqualucci L, Ballon G, Tam W, Nandula SV, Shen Q, et al. Deregulated BCL6 expression recapitulates the pathogenesis of human diffuse large B cell lymphomas in mice. *Cancer Cell* 2005;7:445-55.
6. Harris AW, Pinkert CA, Crawford M, Langdon WY, Brinster RL, Adams JM. The E mu-myc transgenic mouse. A model for high-incidence spontaneous lymphoma and leukemia of early B cells. *J Exp Med* 1988;167:353-71.
7. Limpens J, de Jong D, van Krieken JH, Price CG, Young BD, van Ommen GJ, et al. Bcl-2/JH rearrangements in benign lymphoid tissues with follicular hyperplasia. *Oncogene* 1991;6:2271-6.
8. Yang X, Lee K, Said J, Gong X, Zhang K. Association of Ig/BCL6 translocations with germinal center B lymphocytes in human lymphoid tissues: implications for malignant transformation. *Blood* 2006;108:2006-12.
9. Iqbal J, Neppalli VT, Wright G, Dave BJ, Horsman DE, Rosenwald A, et al. BCL2 expression is a prognostic marker for the activated B-cell-like type of diffuse large B-cell lymphoma. *J Clin Oncol* 2006;24:961-8.
10. Bea S, Zettl A, Wright G, Salaverria I, Jehn P, Moreno V, et al. Diffuse large B-cell lymphoma subgroups have distinct genetic profiles that influence tumor biology and improve gene-expression-based survival prediction. *Blood* 2005;106:3183-90.
11. Tagawa H, Suguro M, Tsuzuki S, Matsuo K, Kaman S, Ohshima K, et al. Comparison of genome profiles for identification of distinct subgroups of diffuse large B-cell lymphoma. *Blood* 2005;106:1770-7.
12. Berglund M, Enblad G, Flordal E, Lui WO, Backlin C, Thunberg U, et al. Chromosomal imbalances in diffuse large B-cell lymphoma detected by comparative genomic hybridization. *Mod Pathol* 2002;15:807-16.
13. Casilli F, Di Rocco ZC, Gad S, Tournier I, Stoppa-Lyonnet D, Frebourg T, et al. Rapid detection of novel BRCA1 rearrangements in high-risk breast-ovarian cancer families using multiplex PCR of short fluorescent fragments. *Hum Mutat* 2002;20:218-26.
14. Killian A, Di Fiore F, Le Pessot F, Blanchard F, Lamy A, Raux G, et al. A simple method for the routine detection of somatic quantitative genetic alterations in colorectal cancer. *Gastroenterology* 2007;132:645-53.
15. Bastard C, Raux G, Fruchart C, Parmentier F, Vaur D, Penther D, et al. Comparison of a quantitative PCR method with FISH for the assessment of the four aneuploidies commonly evaluated in CLL patients. *Leukemia* 2007;21:1460-3.
16. Rovelet-Lecrux A, Hannequin D, Raux G, Le Meur N, Laquerriere A, Vital A, et al. APP locus duplication causes autosomal dominant early-onset Alzheimer disease with cerebral amyloid angiopathy. *Nat Genet* 2006;38:24-6.
17. Rao PH, Houldsworth J, Palanisamy N, Murty VV, Reuter VE, Motzer RJ, et al. Chromosomal amplification is associated with cisplatin resistance of human male germ cell tumors. *Cancer Res* 1998;58:4260-3.
18. Tagawa H, Kaman S, Suzuki R, Matsuo K, Zhang X, Ota A, et al. Genome-wide array-based CGH for mantle cell lymphoma: identification of homozygous deletions of the proapoptotic gene BIM. *Oncogene* 2005;24:1348-58.
19. Quintanilla-Martinez L, Kremer M, Keller G, Nathrath M, Gamboa-Dominguez A, Meneses A, et al. p53 Mutations in nasal natural killer/T-cell lymphoma from Mexico: association with large cell morphology and advanced disease. *Am J Pathol* 2001;159:2095-105.
20. Hans CP, Weisenburger DD, Greiner TC, Gascoyne RD, Delabie J, Ott G, et al. Confirmation of the molecular classification of diffuse large B-cell lymphoma by immunohistochemistry using a tissue microarray. *Blood* 2004;103:275-82.
21. Kwiatkowski F, Girard M, Hacène K, Berlie J. SEM: a suitable statistical software for research in oncology. *Bull Cancer* 2000;87:715-21.
22. Chen W, Houldsworth J, Olshen AB, Nanjangud G, Chaganti S, Venkatraman ES, et al. Array comparative genomic hybridization reveals genomic copy number changes associated with outcome in diffuse large B-cell lymphomas. *Blood* 2006;107:2477-85.
23. Bea S, Colombo L, Lopez-Guillermo A, Salaverria I, Puig X, Pinyol M, et al. Clinicopathologic significance and prognostic value of chromosomal imbalances in diffuse large B-cell lymphomas. *J Clin Oncol* 2004;22:3498-506.
24. Houldsworth J, Olshen AB, Cattoretti G, Donnelly GB, Teruya-Feldstein J, Qin J, et al. Relationship between REL amplification, REL function, and clinical and biologic features in diffuse large B-cell lymphomas. *Blood* 2004;103:1862-8.
25. Houldsworth J, Mathew S, Rao PH, Dyomina K, Louie DC, Parsa N, et al. REL proto-oncogene is frequently amplified in extranodal diffuse large cell lymphoma. *Blood* 1996;87:25-9.
26. Koduru PR, Raju K, Vadmal V, Menezes G, Shah S, Susin M, et al. Correlation between mutation in P53, p53 expression, cytogenetics, histologic type, and survival in patients with B-cell non-Hodgkin's lymphoma. *Blood* 1997;90:4078-91.
27. Winter JN, Weller EA, Horning SJ, Krajewska M, Variakojis D, Habermann TM, et al. Prognostic significance of Bcl-6 protein expression in DLBCL treated with CHOP or R-CHOP: a prospective correlative study. *Blood* 2006;107:4207-13.
28. Mounier N, Briere J, Gisselbrecht C, Emile JF, Lederlin P, Sebban C, et al. Rituximab plus CHOP (R-CHOP) overcomes bcl-2--associated resistance to chemotherapy in elderly patients with diffuse large B-cell lymphoma (DLBCL). *Blood* 2003; 101:4279-84.
29. Mestre-Escorihuela C, Rubio-Moscardo F, Richter JA, Siebert R, Climent J, Fresquet V, et al. Homozygous deletions localize novel tumor suppressor genes in B-cell lymphomas. *Blood* 2007;109:271-80.

Authorship and Disclosures

All the authors made substantial contributions to the conception and design of the study, or acquisition of data, or analysis and interpretation of data, drafting the article or revising it critically for important intellectual content; all approved of the version to be published. The authors reported no potential conflicts of interest.